Iterative Fractionation of Recycling Receptors from Lysosomally Destined Ligands in an Early Sorting Endosome

Kenneth W. Dunn, Timothy E. McGraw, and Frederick R. Maxfield

Departments of Pathology and Physiology, Columbia Univesity, New York 10032

Abstract. To study the fusion and separation of endocytic compartments, we have used digital image analysis to quantify the accumulation of fluorescent ligands in endosomes during continuous endocytosis for periods of 1–20 min. Fluorescently labeled transferrin (Tf) and low density lipoproteins (LDL) were used as markers of recycling receptors and lysosomally directed ligands respectively. By measuring the intensity of individual endosomes, we found that the amount of LDL per endosome increases 30–40-fold between 1 and 10 min and then plateaus. In contrast, the amount of Tf per endosome reaches a steady state within 2 min at a level that is only three to four times that at 1 min.

We used pulse-chase double label methods to demonstrate that Tf cycles through the compartment in which the LDL accumulates. When both Tf and LDL are added to cells simultaneously for 2 min, nearly all endosomes contain both labels. With 2–4 min further incubation in the absence of external ligands, LDL-containing compartments become depleted of Tf as Tf is directed to para-Golgi recycling endosomes. However, if Tf is added to the medium 2–4 min after a pulse with LDL, most of the LDL-containing endosomes become labeled with Tf. The data indicate that at least 30–40 endocytic vesicles containing both Tf and LDL fuse with an endosomal compartment over a period of 5–10 min. LDL accumulates within this compartment and Tf is simultaneously removed. Simple mathematical models suggest that this type of iterative fractionation can lead to very high efficiency sorting.

MAMMALIAN cells internalize a variety of growth factors, nutrients, toxins and viruses through receptor-mediated endocytosis (for review, see Goldstein et al., 1985). After internalization, endocytosed receptors and ligands may be routed in one of several ways. Epidermal growth factor is directed to lysosomes as is its receptor (Carpenter and Cohen, 1979). Transferrin (Tf)[1] unloads its iron and is then recycled back to the cell surface along with its receptor (Dautry-Varsat et al., 1983; Klausner et al., 1983). In polarized cells, ligands and receptors may be transported from one domain of the plasma membrane to another (Mostov et al., 1984; Fuller and Simons, 1986). Internalized asialoglycoproteins (ASGP), α-2-macroglobulin (α_2M), and low density lipoprotein (LDL) are directed to lysosomes and degraded while their receptors are recycled back to the cell surface (Van Leuven et al., 1980; Brown et al., 1983; Breitfeld et al., 1985). Some toxins and viruses enter the cytosol directly from endosomes (Keen et al., 1982; Marsh et al., 1983; Olsnes and Sandvig, 1985). The endocytic pathways of Tf and LDL, the two ligands used in this study, are depicted schematically in Fig. 1. The nomenclature for endocytic compartments is not yet standardized. For consistency with our other papers examining endocytosis in CHO cells, we use here the names shown in Fig. 1. The relationship to some other nomenclature is given in the figure legend.

Despite having different endocytic fates, diferent receptors and ligands are collected into shared coated pits and internalized into the same endocytic vesicles (Maxfield et al., 1978; Pastan and Willingham, 1983). The question then arises of how molecules with different endocytic fates, but residing in the same endosome, are separated from one another and directed onto different intracellular pathways.

For ligands that are separated from their receptors and directed to lysosomes, while their receptors are recycled back to the cell surface, sorting depends in part on the acid-dependent dissociation of receptors from ligands. For this class of ligands (such as α_2M, ASGP, and LDL), the acidification that occurs in endosomes is sufficient to yield dissociation (Tycko et al., 1983; Brown et al., 1983; Harford et al., 1983*a*, 1983*b*) and thus reduces the problem of endocytic sorting to one of separating membrane-bound receptors from ligands dispersed into the endosome lumen. It has long been appreciated that endocytosed membrane itself must be recycled at a high rate, particularly in certain cells that pino-

1. *Abbreviations used in this paper*: ASGP, asialoglycoprotein; dil-LDL, LDL conjugated to 3,3′-dioctadecylindocarbocyanine; diO-LDL, LDL conjugated to 3,3′-dioctadecyloxacarbocyanine; F-α_2M, fluorescein-α_2-macroglobulin; LDL, low density lipoproteins; α_2M, α-2-macroglobulin; MES, 2-[*n*-morpholino]ethanesulfonic acid; R-Tf, human transferrin conjugated to rhodamine; Tf, human transferrin.

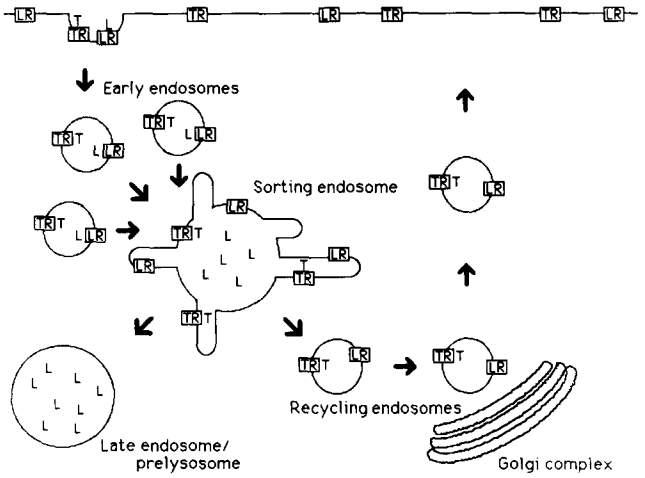

Figure 1. Schematic diagram of the endocytic pathway of internalized diferric Tf (*T*) and LDL (*L*). After binding to specific receptors on the cell surface, ligands are collected into coated pits and internalized together into early endosomes. Later, ligands are found in the larger sorting endosomes, each of which consists of a large vacuole with tubular extensions. From this point receptors and ligands to be recycled are separated from those bound for lysosomes. In this example, the receptor for LDL (*LR*) is shown leaving the sorting endosome for the recycling endosomes, while the LDL itself is next found in the late endosomal/prelysosomal compartment, and later still in lysosomes. In contrast, Tf recycles along with its receptor (*TR*) after releasing iron. Both the receptors for LDL and the apo-Tf receptor–ligand complex are returned to the cell surface via the recycling endosomes that are located near the Golgi complex in CHO cells. The lumenal contents of the sorting endosome may be exported from the sorting endosome onto a lysosomal pathway or the sorting endosome itself may mature into a prelysosomal structure. Similar compartments to the "sorting endosome" have been described in various models of endocytosis as CURL (Geuze et al., 1983), "early endosomes" (Schmid et al., 1988), and "receptosomes" (Pastan and Willingham, 1983). At present there is no standard nomenclature for the different organelles involved in endocytosis. The terminology used in this paper is consistent with previous work from this laboratory (e.g., Salzman and Maxfield, 1989).

cytose vast amounts of plasma membrane (Duncan and Pratten, 1977; Burgert and Thilo, 1983; Steinman et al., 1983).

Receptor recycling occurs with high efficiency. From the kinetics of internalization and degradation, it can be estimated that each LDL receptor recycles 150 times (Goldstein et al., 1985), each Tf receptor up to 300 times (Omary and Trowbridge, 1981), and each ASGP receptor ~250 times (Schwartz and Rup, 1983). These figures suggest that receptors are recycled with >99% efficiency.

Ligands of recycling receptors are sorted to lysosomes with somewhat lower efficiency. Between 25% and 50% of internalized ASGP is returned intact to the cell surface of rat hepatocytes (Weigel and Oka, 1984) and between 28% and 50% of internalized ASGP is returned intact to the cell surface of HepG2 cells (Simmons and Schwartz, 1984). Yamashiro et al. (1984) found only ~80% of the α_2M internalized by CHO cells was directed onto a lysosomal pathway after sorting from its receptor. Up to 10% of endocytosed LDL is returned intact to the cell surface of skin fibroblasts (Greenspan and St. Clair, 1984).

Sorting may be accomplished in one of two ways. In the first, sorting may occur in a single, very efficient step. Linderman and Lauffenburger (1988) developed mathematical descriptions for a model of this type in which recycling components migrate freely throughout the membrane of the sorting endosome, but are trapped in tubules from which recycling vesicles form. Sorting efficiency for a given receptor would be a function of how freely and rapidly it enters tubules. Lumenal ligands accumulate in the sorting endosome

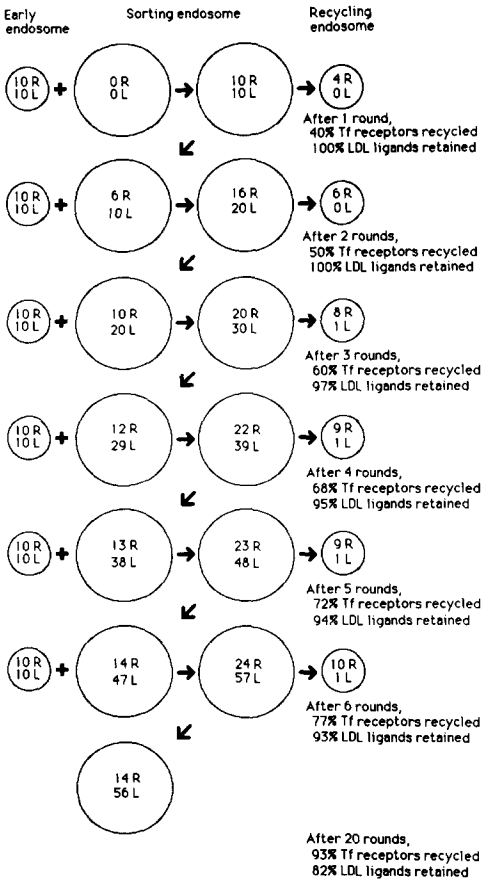

Figure 2. Schematic diagram of the iterative fractionation model of endocytic sorting. In this example, we assume that the sorting endosome fuses continuously with early endosomes, each of which carries 10 receptor and 10 ligand molecules. After fusion, receptors are free to migrate over the membrane, and ligands are free to disperse throughout the lumen of the sorting endosome. Simultaneously (although not necessarily in the lockstep depicted here) 40% of the receptors and 2% of the ligand contained in the sorting endosome are sorted and exported via each recycling vesicle. As shown in the running budget at the right of the figure, receptor recycling efficiency increases and ligand retention efficiency decreases with each round of sorting. One can also see that although the sorting endosome exports only 40% of its receptors with each sorting step, the sorting endosome is operating at 100% efficiency after six rounds of sorting since from this point onward the number of receptors exported in each round equals the number imported in that round. For simplicity, we have depicted the iterative fractionation sorting model as if the processes of fusion and sorting are linked, but this need not be the case. If recycling vesicles continue to form after fusion has stopped, recycling receptors may continue to be exported from the sorting endosome and the number delivered to lysosomes further decreased.

and are eventually degraded along with whatever receptors have been left behind at the time of sorting.

Alternatively, sorting may be accomplished in a more continuous fashion by many iterations of a sorting step. The sorting step need not be particularly efficient since, like a fractional distillation apparatus, high efficiency sorting would result from repetition of the sorting step.

These two types of models lead to specific and different predictions about the accumulation of recycling and lysosomally directed ligands in the sorting compartment. In the first process, both types of ligands would accumulate in endosomes simultaneously and with similar kinetics until the separation process began. This could occur after repeated fusions of coated pit-derived vesicles (early endosomes). It could also occur separately for each of these early endosomes, as would be required in models of endocytosis in which no mixing occurs between sequentially endocytosed molecules (Ajioka and Kaplan, 1987; Ward et al., 1989). In the second type of process, the sorting compartment would experience repeated fusions with vesicles containing newly endocytosed ligands, while simultaneously exporting recycling components and accumulating lysosomally directed ligand. In this type of process, lysosomally directed ligands would accumulate to a greater degree in the sorting compartment than the recycling ligands and receptors. Also, a steady-state level of recycling ligands in the sorting compartment would be achieved more rapidly. Finally, the sorting compartment should be capable of fusion with newly endocytosed material for several minutes. This type of iterative fractionation is illustrated schematically in Fig. 2.

Support for the notion that the process of endocytic sorting involves large numbers of early endosome fusions comes from data obtained both in vivo (Salzman and Maxfield, 1988, 1989) and in vitro (Gruenberg and Howell, 1986; Braell, 1987; Diaz et al., 1988), which show that at early times endosomes are fusogenic but they may lose their capacity for fusion with time. In electron microscopic examinations of hepatocytes, Geuze et al. (1983) observed that endosomes increased in size while accumulating ASGP, suggesting repeated fusion of early endosomes.

Endosome fusion could be compatibile with either of the two types of sorting models described above. In this paper, we describe experiments using digital image processing to measure the accumulation of Tf and LDL in endosomes. The data obtained are consistent with the iterative fractionation model.

Materials and Methods

Cell Cultures

TRVb-1 cells, a CHO cell line lacking endogenous Tf receptor activity and expressing transfected human Tf receptor (McGraw et al., 1987) were cultured on plastic tissue culture dishes in bicarbonate buffered F-12 supplemented with 5% FCS (Gibco Laboratories, Grand Island, NY; 100 U/ml penicillin and 100 μg/ml streptomycin at 37°C in a 5% CO_2 humidified air atmosphere. Cells were passaged by trypsinization.

2 d before each experiment cells were plated onto cover slip bottom dishes, 35-mm plastic tissue culture dishes whose bottoms have been replaced with polylysine coated glass coverslips (Salzman and Maxfield, 1988). 1 d before each experiment, the culture medium of each was replaced with a similar medium but made with 5% delipidated FCS to stimulate increased expression of the cells' LDL receptors (Goldstein et al., 1983).

Fluorescent Ligand Preparation

Human Tf (Sigma Chemical Co., St. Louis, MO) was iron loaded, further purified by Sephacryl S-300 gel filtration and conjugated to rhodamine as previously described (Yamashiro et al., 1984). LDL was prepared from whole human serum as described by Goldstein et al. (1983). LDL conjugated to 3,3'-dioctadecylindocarbocyanine (DiI-LDL) and 3,3'-dioctadecyloxacarbocyanine (diO-LDL), (Molecular Probes, Eugene, OR) were prepared as described by Pitas et al. (1981). Fluorescent LDLs were kindly provided by Dr. Ira Tabas (Columbia University).

Fluorescent Labeling of Cells

5 min before labeling, the culture medium of each coverslip bottom dish was replaced with F-12 without bicarbonate, buffered with 20 mM Hepes (pH 7.4), supplemented with 100 U/ml penicillin, 100 μg/ml streptomycin and 2 mg/ml ovalbumin (Sigma Chemical Co.) and incubated in air on a warm tray at 37°C. Cells were rinsed in the same medium and then incubated with either 5 μg/ml DiI-LDL or 20 μg/ml rhodamine-Tf (R-Tf) in the Hepes-buffered F-12 medium described above in air, on a warm tray at 37°C. At the end of the incubation period, cells were rapidly rinsed four times in medium 1 (150 mM NaCl, 20 mM Hepes, pH 7.4, 1 mM $CaCl_2$, 5 mM KCl, 1 mM $MgCl_2$), two times in a mild acid solution of 50 mM MES (2-[*n*-morpholino] ethanesulfonic acid), 280 mM sucrose, pH 5.0, 4 times in medium 1, fixed for 2 min at room temperature in 2% formaldehyde freshly diluted in medium 1, rinsed four times in medium 1 and placed in darkness until used. For double label studies, cells were incubated in medium 1 supplemented with 2 mg/ml ovalbumin, 5 μg/ml diO-LDL and/or 20 μg/ml R-Tf for the indicated times. In pulse-chase studies cells were rinsed free of label(s) with five changes of medium 1 before the chase in unlabeled medium 1 with 2 mg/ml ovalbumin. In those studies where cells were treated with second label following the chase interval, cells were rinsed four more times at the end of the chase, before administration of the second label. In all dual label studies, cells were immediately chilled at the end of incubations, rinsed four times in ice-cold medium 1, 2 times in ice-cold mild acid solution and another four times in ice-cold medium 1. Cells were then fixed on ice as described above.

Fluorescence Microscopy

R-Tf and diI-LDL were visualized using a fluorescence microscope (Diavert, E. Leitz, Inc., Rockleigh, NJ) equipped with a 63×, NA 1.4 objective, a 530–560-nm band pass excitation filter, a 580-nm dichroic mirror and 580-nm-long pass emission filter. diO-LDL was visualized with the same equipment but with a 450–490-nm band pass excitation filter, a 510-nm dichroic mirror and a 515-nm-long pass emission filter. Images were recorded on a video cassette recorder (CR6650U; JVC (Elmwood Park, NJ)) with a camera and image intensifier (model No. VS2000N and KS1380, respectively; Videoscope International, Ltd., Washington D.C.). Neutral density excitation filters (50%, 25%, 10%, 5%, 2.5% transmission) were used to keep fluorescence intensities from exceeding the camera's linear range. The image intensifier was kept at one gain setting for all time point recordings for each ligand. Fields were chosen under bright field illumination. For each field, 10 serial focal plane images were recorded, 1.2-μm apart, for ~2 sec apiece. Focal plane adjustment was made using a microstepping motor z-axis controller (Kinetek Corp., Yonkers, NY).

Image Processing

We developed a procedure for automatically measuring the fluorescence intensity of individual endosomes throughout a cell. This required a method for identifying endosomes against background fluorescence, finding the in-focus plane for each endosome, separating the fluorescent image of each endosome from those of nearby endosomes and measuring the intensity of each resolved endosome.

Images were digitized and background corrected as described previously (Maxfield, 1989; Maxfield and Dunn, 1989) with the following changes: digital images were constructed from the average of 16 video frames, only the central 312 × 312 pixel region of the original 512 × 512 pixel image was analyzed and background intensity for each pixel was calculated as the median intensity in a surrounding 32 × 32 pixel region (5.5 × 5.5 μm). This procedure does not lead to any significant subtraction of label fluorescence from in-focus endosomes since all pixels within an endosome are above the median intensity in the region (Maxfield and Dunn, 1989). This has been verified for endosomes under all conditions in this paper.

To distinguish partially overlapping images of closely adjacent fluores-

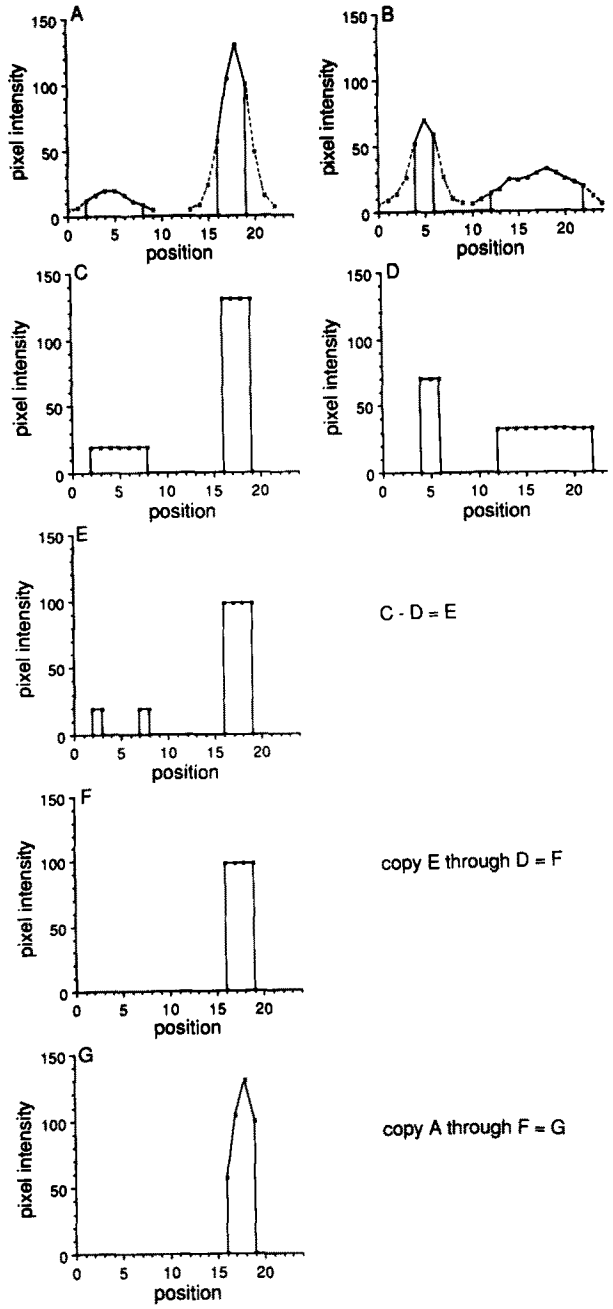

Figure 3. Schematic diagram of image focus correction procedure. This figure shows fluorescence intensity profiles through the centers of two endosomes in two adjacent focal planes. The procedure illustrated is used to determine if an endosome is in focus in the image from which the intensity profile (*A*) was obtained by comparing it with the adjacent focal plane (*B*). Each profile has both a focused (*tall and narrow*) and a blurred, out-of-focus spot (*short and wide*). A spot is defined as a group of contiguous pixels whose brightness is above a threshold value. The purpose of the method in this example is to delete the left spot of image *A*, while retaining the measured pixels of the right spot. Before focal correction, pixels whose intensities are <40% of that of the brightest pixel in each spot (i.e., those shown by the dashed line) are deleted. The first step of this process requires that the maximum intensity of each spot be determined and assigned to all pixels in the spot. The results of this operation on images *A* and *B* are shown in profiles *C* and *D*, respectively. Next the intensities of image *D* are subtracted, pixel-by-pixel, from those of image *C*. The profile of the remainder image is shown as profile *E*. Image *E* is then copied, using the nonzero pixels of image *D* as a stencil, to make image *F*. Finally image *A*, the original image to be processed, is copied through the nonzero pixels of image *F* to yield image *G*. As can be seen from the profiles, the out-of-focus spot has been removed from the original image, leaving only the focused spot. The procedure is then repeated using the other adjacent out-of-focus focal plane image.

cent endosomes, an automated procedure was employed that removed the relatively dim areas of overlap by blackening pixels whose brightness level is <40% of that of the brightest pixel found in the same spot (a spot being defined as a group of contiguous pixels whose brightness is above a threshold value).

To quantify the fluorescence intensity of each individual endosome we devised a procedure for identifying the in-focus focal plane for each endosome from a series of optical sections. We determined that fluorescent endosomes would behave almost like point sources of light in our system since fluorescent beads ranging in diameter from 0.1 to 0.9 μm (Polysciences Inc., Warrington, PA) and fluorescent endosomes all produce images of nearly the same size and intensity profile shape. In principle, the integrated fluorescence intensity of a point source (like an endosome) is nearly independent of focal plane within the microscope's focal range (Kam, 1987). The problem becomes one of resolution, however, as out of focus images merge into one another and fade into the background fluorescence. Out-of-focus contributions to an image may be eliminated either mathematically, using the point spread function of the microscope/detector system, or optically, using a confocal microscope (Kam, 1987). Our technique makes use of the simplest aspect of the point spread function: the image of a point source becomes both broader and dimmer as the distance from the focal plane increases. The process is depicted schematically and described fully in Fig. 3. Briefly, fluorescent images were recorded for 10 serial focal planes (1.2 μm apart) that spanned each field of cells. Images were next processed as described above. Each focal plane image was then compared to the images of the adjacent two focal planes. An endosome was judged to be in focus in a given focal plane if it was present in both adjacent focal planes, and had a lower fluorescence intensity in both adjacent focal planes. If an endosome was either not present, or was brighter in one of the adjacent focal planes, it was discarded from the focal plane being analyzed. This procedure was repeated for the inner eight focal planes of each field and the resultant images were combined to yield a composite image of focused endosomes. At this point, fluorescent spots whose sizes fall outside the range observed for a single endosome (between 4 and 40 pixels in area) were deleted from images. Large spots resulted from the inability of the method to distinguish the images of closely adjacent endosomes. The brightness of each endosome was quantified as the sum of the brightness values of all pixels whose brightness was at least 50% of that of the brightest pixel in the endosome image, a parameter that was found to be relatively insensitive to focus errors. Measurements of serial focal plane images (taken at 0.1-μm intervals) of 0.13 μm fluorescent microspheres showed that measured intensity errors of ~10% could be expected for slightly out-of-focus endosomes.

Results

TRVb-1 cells incubated with 5 μg/ml of diO-LDL and 20 μg/ml R-Tf for 2 min and fixed immediately show a vesicular pattern of fluorescence in which nearly all endosomes containing LDL also contain Tf (Fig. 4, *a* and *b*). Between 2 and 4 min of further incubation in the absence of fluorescent ligands Tf leaves the LDL-containing compartments and accumulates in the para-Golgi region (Fig. 4, *c*, *d*, *e*, and *f*). During this same period of time, however, the LDL-containing compartments are capable of receiving newly endocytosed Tf (Fig. 5, *a* and *b*), indicating that Tf is continuously cycling through these compartments. LDL-containing endosomes lose the capacity for fusion with time, so that very few are accessible to Tf endocytosed following an 8-min chase (Fig. 5, *c* and *d*).

When cells are continuously exposed to both R-Tf and diO-LDL for 10 min several different classes of endosomes can be identified (Fig. 6). Recycling endosomes, characterized

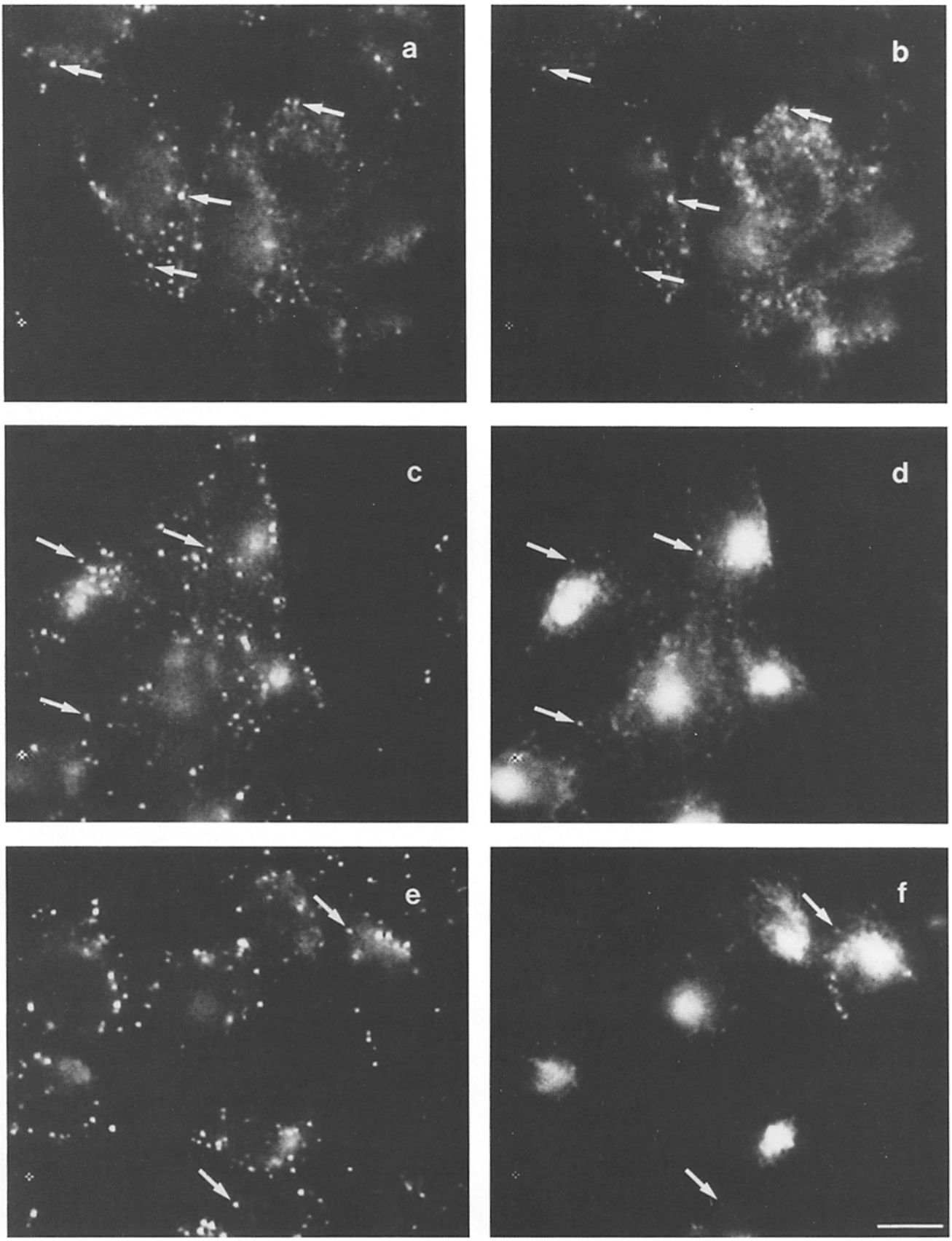

Figure 4. Movement of R-Tf through the sorting endosome. TRVb-1 cells were incubated in 5 μg/ml diO-LDL and 20 μg/ml R-Tf for 2 min and either fixed immediately (*a* and *b*), rinsed and incubated for another 2 min in the absence of labels (*c* and *d*), or rinsed and incubated for another 4 min in the absence of labels (*e* and *f*). *a*, *c*, and *e* were obtained using fluorescein optics to display diO-LDL. *b*, *d*, and *f* were obtained using rhodamine optics to display R-Tf. Arrows indicate examples of endosomes containing both ligands. Using the arrows as landmarks, one can see that with time Tf appears to depart from the LDL-containing endosomes as it accumulates in the para-Golgi region. Bar, 10 μm.

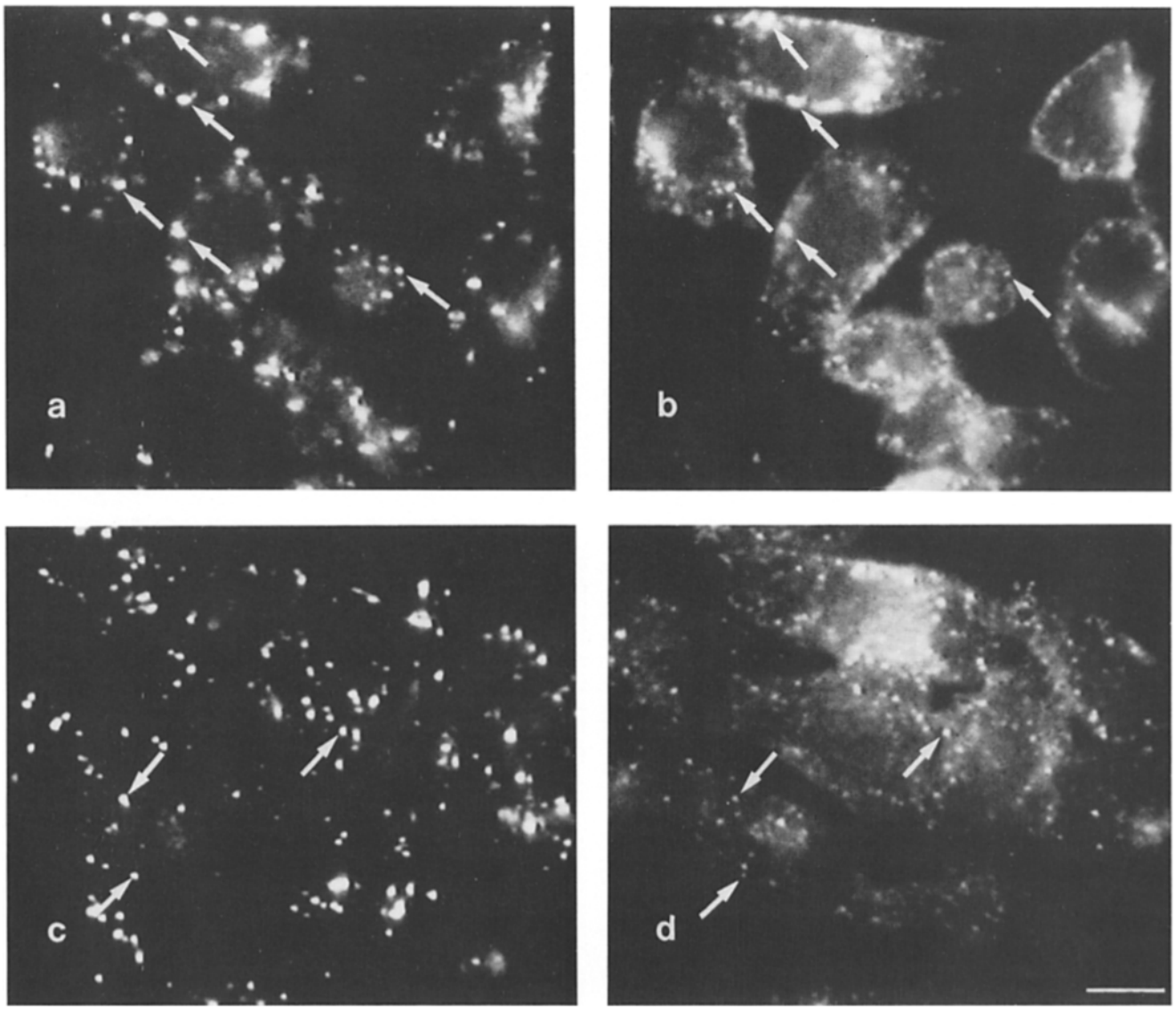

Figure 5. Time-dependent loss of fusion competence by the sorting endosome. TRVb-1 cells were incubated in 5 μg/ml diO-LDL for 2 min, rinsed, and incubated in the absence of label for either 2 min (*a* and *b*) or 8 min (*c* and *d*), rinsed, and incubated in 20 μg/ml R-Tf for 2 min. As in Fig. 4, diO-LDL fluorescence is displayed in panels *a* and *c*, R-Tf fluorescence is displayed in *b* and *d*. Arrows indicate examples of endosomes containing both ligands. Using the arrows as landmarks, one can see that while most of the diO-LDL–containing endosomes can be labeled with Tf endocytosed 2 min later, very few are accessible to Tf endocytosed 8 min later. Bar, 10 μm.

by the presence of Tf and absence of LDL, accumulate in the para-Golgi region. Late endosomes, which contain LDL but not Tf, distribute in a punctate pattern. Sorting endosomes, which contain both Tf and LDL, also show a punctate pattern. Endosomes containing diO-LDL display a wide range of fluorescence intensities, only an upper fraction of which is shown here because of the limited dynamic range of the video camera. As shown below, this variation in fluorescence intensity results from the accumulation of LDL in individual endosomes with time of incubation. R-Tf can be found in endosomes showing every level of diO-LDL accumulation and, in particular, in endosomes with the largest accumulation of diO-LDL, indicating that Tf cycles through the LDL accumulating compartment, which can be functionally defined as a sorting endosome.

To measure the kinetics of accumulation of receptors and ligands in endosomes, we have developed a method for measuring the relative amounts of fluorescently labeled ligands in individual endosomes by quantifying their fluorescence intensity (see Materials and Methods). In this procedure TRVb-1 cells were incubated for various periods of time with either 5 μg/ml of diI-LDL (a fluorescent ligand delivered mainly to lysosomes) or 20 μg/ml of R-Tf (a fluorescent recycling receptor marker). Cells were then fixed in 2% formaldehyde and their fluorescent images videotaped. The time course of accumulation of diI-LDL or R-Tf in endosomes was quantified as the increase in individual endosome brightness with time of incubation.

Measuring fluorescence intensity of individual endosomes required developing techniques capable of quantifying fluorescence intensity over a 1,000-fold range, capable of minimizing the effects of focal plane on endosome image fluores-

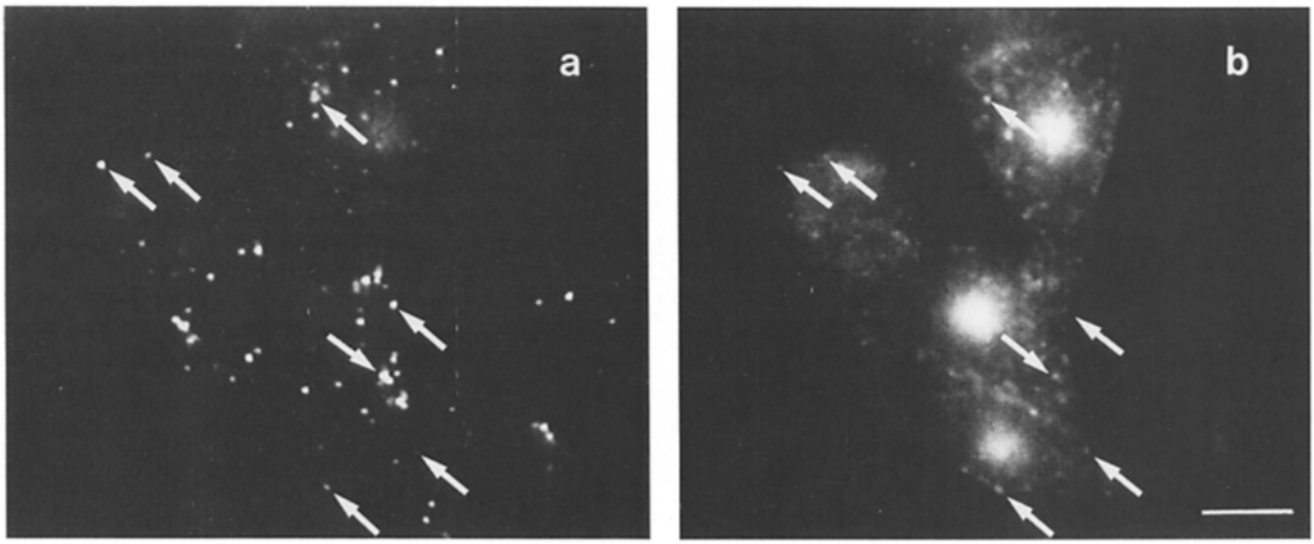

Figure 6. Access of R-Tf to an LDL-accumulating sorting endosome. TRVb-1 cells were incubated in 5 μg/ml diO-LDL and 20 μg/ml R-Tf for 10 min. DiO-LDL fluorescence is shown in *a*, and R-Tf fluorescence is shown in *b*. Arrows indicate examples of endosomes containing both ligands. Note that R-Tf occurs in endosomes containing a range of quantities of diO-LDL, including those with the largest accumulation of diO-LDL. Bar, 10 μm.

cence and capable of making large numbers of measurements. To extend the range of measurement, neutral density filters were placed in the excitation path, effectively extending the video camera's linear sensitivity range 40-fold. Since we were interested in measuring the brightness of the brightest endosomes under each experimental condition, the dimmest endosomes were necessarily attenuated to a brightness level below the camera's sensitivity. Since the measured fluorescence intensity of an endosome is a function of focal plane,

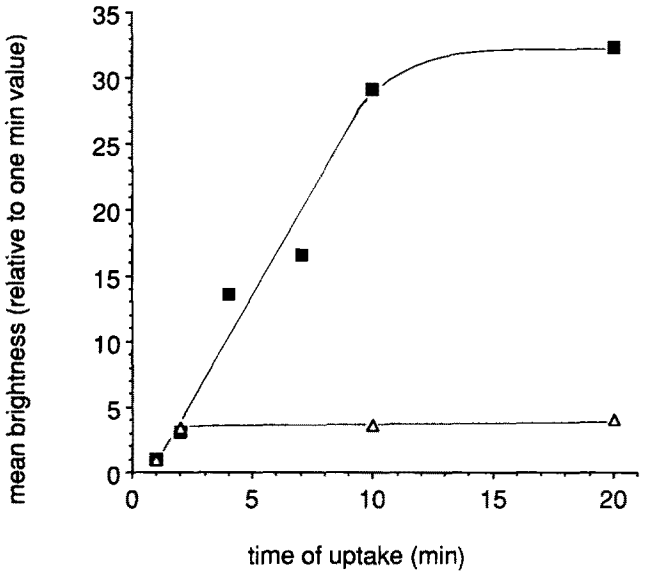

Figure 7. Time course of dil-LDL and R-Tf accumulation in endosomes. Cells were continuously labeled with either 5 μg/ml DiI-LDL (*squares*) or 20 μg/ml R-Tf (*triangles*) for the indicated periods of time and the brightnesses of the endosomes quantified as described. Points shown are mean measured endosome brightnesses (relative to the 1-min value) of four fields of ~3–5 cells each. Standard errors of the mean are in each case smaller than the symbol size.

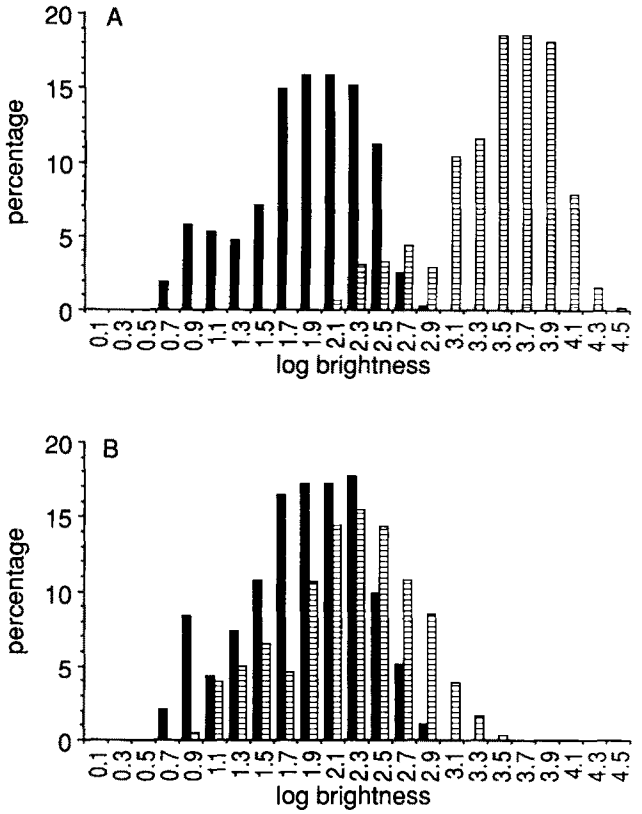

Figure 8. The frequency distributions of endosome brightnesses (arbitrary units) for TRVb-1 cells incubated with dil-LDL (*A*) or R-Tf (*B*). Cells were incubated for either 1 min (*solid bars*) or 10 min (*lined bars*). Each distribution represents the combined data of 10 fields of ~3–5 cells each (totaling between 470 and 980 endosomes for each distribution). The mean brightness of dil-LDL containing endosomes increases 37-fold, while the mean brightness of R-Tf containing endosomes increases by 2.5 times.

a method was developed to eliminate out-of-focus endosomes from an image before measurement. This procedure guaranteed that measurements were made only on those endosomes whose images were recorded within 0.6 μm of the in-focus focal plane. The automated procedure devised to perform this function was capable of rapidly processing large numbers of fluorescent images and was, in all cases tested, successful in eliminating endosomes that were judged to be out of focus. Endosome brightness was quantified as the sum of the brightness values of all pixels whose brightness was at least 50% of that of the brightest pixel in the endosome. This parameter is relatively insensitive to focal plane since the integrated fluorescence intensity of a point source is nearly independent of focal plane (Kam, 1987). Measurements of serial focal plane images of fluorescent microspheres showed that errors in intensity measurements arising from misfocus were reduced to ~10% by these procedures (see Materials and Methods). Although recycling ligands (e.g., Tf) and lysosomally directed ligands (e.g., LDL) may be distributed to different regions of the sorting endosome, this should not affect measurements since the shapes of the intensity profiles of endosomes containing either Tf or LDL are indistinguishable from one another.

In CHO and TRVb-1 cells, Tf collects in recycling endosomes that are concentrated in a para-Golgi location after passage through the sorting endosome (Yamashiro et al., 1984; McGraw et al., 1987). Since the para-Golgi concentration of Tf appears as a large mass in fluorescent images of cells, a maximum size criterion applied to eliminate overlapping endosomes (see Materials and Methods) effectively eliminated the postsorting para-Golgi structure from images before quantification. As reported for other lysosomally directed ligands, dil-LDL never shows this pattern, distributing instead in a punctate pattern. Eliminating the para-Golgi Tf accumulation from images will not affect measurements of intensities in the sorting endosome since Tf accumulates in the para-Golgi region only after segregation from lysosomally directed ligands.

To measure the accumulation of LDL in endosomes, TRVbl cells were incubated in medium containing 5 μg/ml dil-LDL for varying periods of time. The cells were rinsed, fixed, and the average endosome brightness determined at each time point. As shown in Fig. 7, measured endosome brightnesses increased almost linearly for 10 min before leveling off. By 10 min the average measured endosome brightness was 30 times the level at 1 min, indicating that these endosomes experienced at least 30 fusions during this interval of time.

In equivalent experiments in which cells were labeled with 20 μg/ml R-Tf, we found that the pattern and extent of R-Tf accumulation in punctate endosomes contrasted sharply with that of dil-LDL. As in cells labeled with dil-LDL, the average measured endosome brightness of R-Tf labeled cells increased approximately fourfold between 1 and 2 min of uptake, but while endosomes of dil-LDL labeled cells continued to brighten at approximately the same rate, R-Tf–containing endosomes stopped increasing in brightness at this point. From 2 min of incubation onward, the para-Golgi recycling structure became prominently labeled with R-Tf.

In a separate experiment, TRVb-1 cells were incubated with fluorescent ligands for either 1 or 10 min. Fig. 8 shows the distribution of measured brightnesses of dil-LDL– and R-Tf–containing endosomes in these cells. In this experiment dil-LDL–containing endosomes increased in brightness by 37 times between 1 and 10 min of continuous uptake, while the brightness of endosomes containing R-Tf increased by only 2.5 times. Fig. 9 shows pseudocolored examples of typical fields of cells from this experiment.

Discussion

While it is generally observed that the amount of internalized ligand increases with time of incubation, the accumulation in individual endosomes has not been investigated quantitatively. The data shown here demostrate that much of the initial increase in intensity during incubation with fluorescent LDL results from an increase in the brightness of individual endosomes, rather than from an increase in number of fluorescently labeled endosomes. Our observation that individual endosomes increase in brightness by 30–40 times during a continuous uptake of dil-LDL clearly indicates that endosomes experience a large number of fusions, suggesting that endosome fusion is a significant aspect of the endocytic process. We have demonstrated that LDL accumulates in a compartment that is accessible to endocytosed Tf (Fig. 6). Although dil-LDL accumulates in these endosomes for 10 min, R-Tf reaches a steady-state level within 2 min. Since LDL and Tf are delivered to this endosome together, the difference in accumulation kinetics indicates that the endosome continuously releases R-Tf but retains dil-LDL and thus acts as a sorting endosome. The simplest explanation for these observations is provided by an iterative fractionation model of sorting.

For illustrative purposes we depicted a simple form of this model in Fig. 2. To analyze the general properties of iterative sorting we used this same simplified model to calculate the accumulation kinetics and overall sorting efficiencies using a range of step-wise sorting efficiency values. The results are shown in Fig. 10 where F is defined as the step-wise sorting efficiency (the fraction of receptors or ligands exported from the sorting endosome with each sorting step). As shown in this figure, the iterative fractionation model predicts that the accumulation of recycling receptors in the sorting endosome would rapidly reach a relatively low steady-state value, but ligands that were retained would continue to accumulate for a longer time and to a much greater degree. In contrast, if the sorting process is not iterative, but occurs in a single maturation step for each sorting endosome (as discussed in the Introduction), both recycling receptors and lysosomally directed molecules would accumulate equally until they were sorted from each other. As shown in Figs. 7 and 8, the accumulation kinetics for LDL and Tf are consistent with the iterative fractionation model.

In an iterative fractionation process, such as that illustrated in Fig. 2, the sorting endosome must continue to fuse with new early endosomes as it exports recycling molecules. These properties were directly demonstrated in the pulse-chase and pulse-chase-pulse experiments in Figs. 4 and 5. When R-Tf and diO-LDL are cointernalized for 2 min, most of the endosomes show the presence of both ligands. With 2 min of chase in the absence of external ligand, the LDL-containing endosomes become depleted of R-Tf and by 4 min almost none contain detectable R-Tf. By 4 min nearly all of the R-Tf has moved to recycling endosomes in the para-Golgi region. These data are in excellent agreement with the

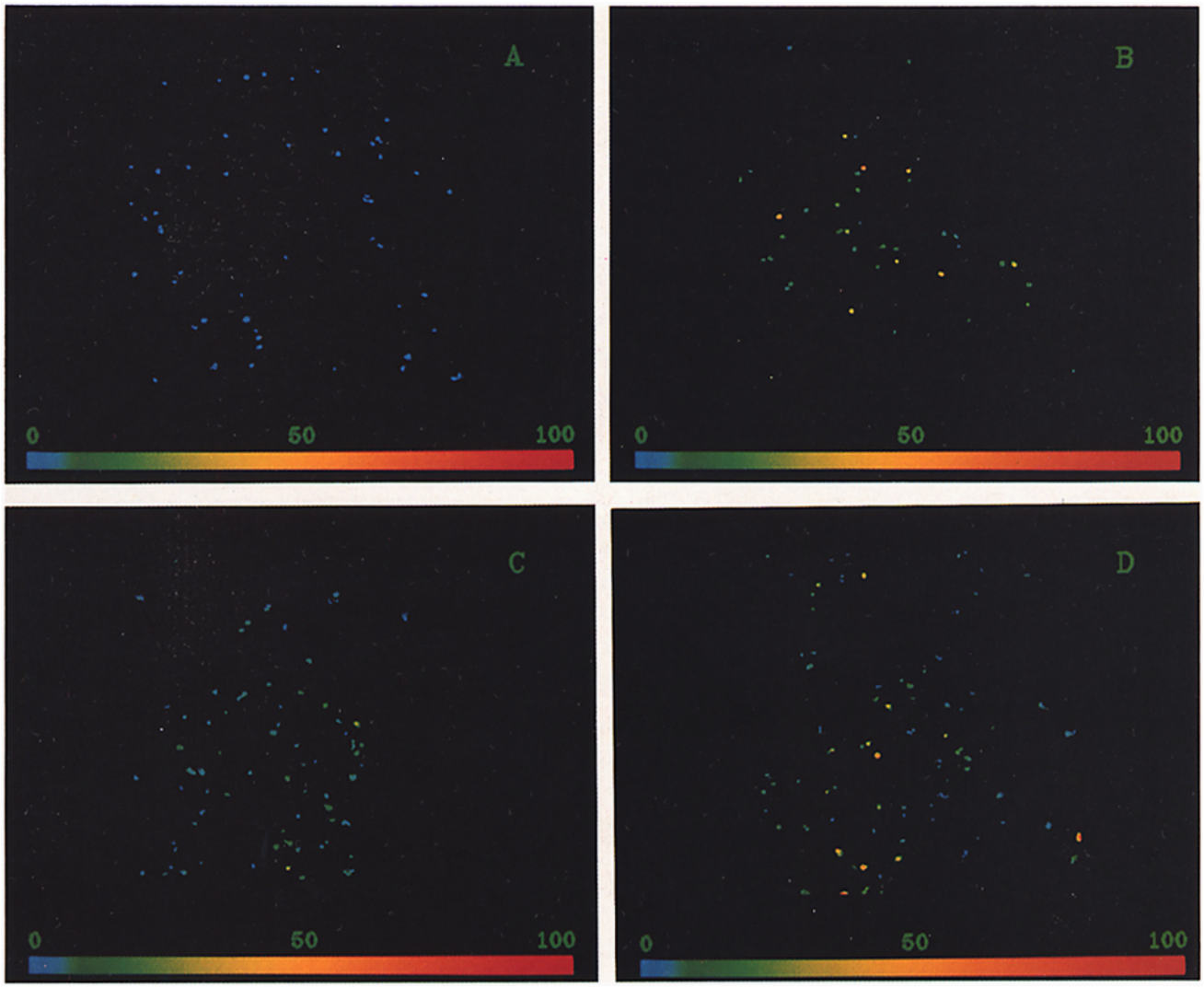

Figure 9. Representative fields from the experiment summarized in Fig. 8. (*A*) 1 min of dil-LDL uptake; (*B*) 10 min of dil-LDL uptake; (*C*) 1 min of R-Tf uptake; (*D*) 10 min of R-Tf uptake. The brightnesses of the images shown have been corrected for the different neutral density filters used in each (*A*, 100% transmission; *B*, 5%; *C*, 100%; *D*, 50%). Images shown have been pseudocolored to facilitate brightness comparisons. The pseudocolor brightness scale is shown at the bottom of each figure. For each ligand, the same pseudocolor conversion was applied for each pair of images. Brightnesses were scaled such that the brightest pixel in the pair had an arbitrary brightness level of 100. Colorbar, 87 μm.

findings of Stoorvogel et al. (1987) that showed that Tf is rapidly segregated from ASGP when the two ligands are cointernalized. The LDL-containing vesicles retain the ability to fuse with new endosomes for several minutes as shown in Fig. 5. Thus, LDL accumulates in an endosome that rapidly exports Tf but continues to fuse with new endosomes. These are the properties required of a sorting endosome in the iterative fractionation model.

The sorting endosome does not continue to fuse with new endosomes indefinitely. As shown in Fig. 5, only a small percentage of endosomes which had been labeled with diO-LDL were still accessible after an 8-min chase. Also, the amount of LDL per endosome does not increase after ~10 min (Fig. 7). The time-dependent loss of fusion accessibility of a sorting endosome has been established by an independent method (Salzman and Maxfield, 1989). In those studies, cells were first allowed to endocytose fluorescein-α_2-macroglobulin (F-α_2M), were then incubated for different periods in unlabeled medium, and then were incubated in medium containing an antifluorescein antibody that quenches fluorescein fluorescence upon binding. The degree of fluorescence quenching is a measure of endosome fusion since the antibody quenches fluorescein fluorescence if and only if it reaches compartments containing F-α_2M. It was found that the compartment containing F-α_2M loses its accessibility to subsequently endocytosed antibody with a half time of 8 min. This suggests that the sorting endosome has an average lifespan of ~8 min. The 10-min period during which dil-LDL accumulates is in good agreement with the 8-min period during which the sorting endosome remains fusion accessible.

An iterative fractionation model can reconcile data that seem to be in conflict according to a single step sorting paradigm. Ajioka and Kaplan (1987) showed that Tf receptors internalized at different times do not intermix. However, Salz-

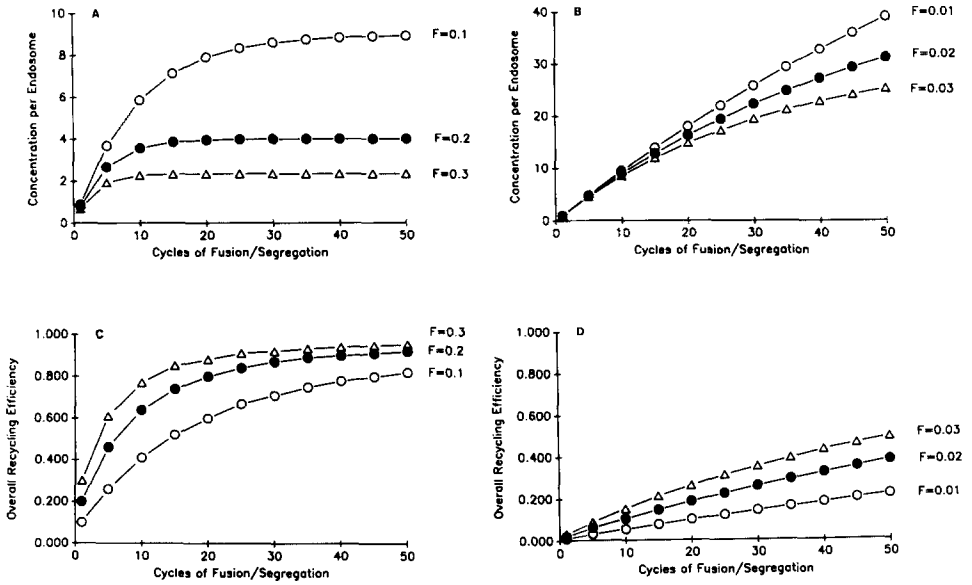

Figure 10. Accumulation kinetics and sorting efficiencies produced through iterative fractionation endocytic sorting. In these figures, the simplified model depicted in Fig. 2 has been used to show how overall receptor recycling efficiency would increase and how ligands would accumulate in the sorting endosome with the number of cycles of fusion/segregation. In each case, F represents the step-wise sorting efficiency (the fraction of receptors or ligands exported from the sorting endosome with each sorting step). Across a range of relatively low values of F (F = 0.1–0.3), the model predicts that, with sufficient repetition, membrane-bound receptors would recycle with high efficiency (*C*), with very little intracellular accumulation (*A*). Assuming small values for the volumes of the recycling vesicles (F = 0.01–0.03) results in large accumulation of lumenal ligand in the sorting endosome (*B*) with minimal delivery to the recycling pathway (*D*). As in Fig. 2, we have, for simplicity, depicted the iterative fractionation sorting process as if the processes of fusion and sorting are linked, but this need not be the case. If recycling vesicles continue to form after fusion has stopped, recycling receptors may continue to be exported from the sorting endosome and recycling efficiency further increased.

man and Maxfield (1988, 1989) have shown that there is substantial fusion of sequentially endocytosed molecules. In the iterative fractionation model, Tf is rapidly removed from the sorting endosome, so previously endocytosed Tf receptors would not still be present when a second pulse of Tf receptors entered the cell.

Although we cannot make an exact determination, we may derive a minimum estimate for the number of fusions experienced by the sorting endosome from the accumulation factors found for dil-LDL. The 30–40-fold increase in the amount of dil-LDL in each sorting endosome between 1 and 10 min of internalization means that the sorting endosome must experience no fewer than 30–40 fusions with early endosomes. To the degree that 1-min-old endosomes result from fusions themselves, and to the degree that dil-LDL is recycled, the actual number of fusions would be correspondingly higher. As shown in Fig. 10, 30 cycles of fusion and budding of vesicles would provide highly efficient recycling even if each cycle were only 20–30% efficient.

A mechanism of sorting is suggested by the tubulovesicular structure of the sorting endosome as shown in electron micrographs (Geuze et al., 1983, 1987). This endosome, called compartment of uncoupling of receptor and ligand (CURL) by Geuze et al., contains both receptors and ligands, but while receptors are largely found in the tubular domain, ligands are primarily found in the vesicular domain. Rome (1985) noted that because of the high surface-area-to-volume ratio of the tubular domain, tubules will contain a disproportionately large amount of membrane-bound receptors while the vesicular portion of the sorting endosome will contain disproportionately more of the lumenal ligand. He suggested that if ligands freely disperse throughout the lumen and receptors freely migrate on the membrane of the sorting endosome, sorting of receptors from ligands may be accomplished by the formation of vesicles from tubules. Such vesicles will have a higher surface-area-to-volume ratio than that of the sorting endosome and will thus withdraw a relatively large amount of membrane-bound receptors with relatively little ligand. With a high enough number of iterations, even the relatively low efficiency of a sorting process resulting purely from geometry could provide a high overall efficiency of recycling. The efficiency of sorting may be further enhanced by preferential direction of some membrane proteins to the tubular portion of the sorting endosome as has been reported for the ASGP receptor (Geuze et al., 1987). Our data do not exclude the possibility that each sorting step could be highly efficient (for example, by clustering of receptors in tubules). However, for step-wise sorting efficiency values <1.0, the overall sorting efficiency is enhanced by iteration of the process.

If the mechanism of sorting is provided by the geometry of the sorting endosome, then bulk membrane should be predominantly sorted to the same recycling compartments as recycling receptors. Koval and Pagano (1989) have found that fluorescent lipid analogues introduced into the plasma membrane and subsequently endocytosed by Chinese hamster ovary (CHO) cells recycle efficiently back to the cell surface apparently via the same compartment as endocytosed Tf (although perhaps with slower kinetics). Since the majority of cell surface proteins probably recycle after endocytosis (Burgert and Thilo, 1983; Raub et al., 1986), it seems likely that the recycling pathway is the default endocytic pathway for membrane proteins. An iterative fractionation process such as that described here would provide a simple and efficient mechanism for recycling lipid and membrane proteins back to the cell surface. Rather than requiring specific signals to recycle, membrane proteins may require specific signals or characteristics (such as aggregation upon ligand binding) to be routed to lysosomes.

While the iterative fractionation model provides a satisfac-

tory mechanism for the sorting of lysosomally directed ligands such as LDL, α_2M and ASGP from their recycling receptors, it is clear that membrane association is not sufficient to ensure recycling of receptors. When Tf receptors (Hopkins and Trowbridge, 1983; Weissman et al., 1986), Fc receptors (Mellman and Plutner, 1984), LDL receptors (Anderson et al., 1982), ASGP receptors (Schwartz et al., 1986), and mannose-6-phosphate receptors (Von Figura et al., 1984) are cross-linked with multivalent antibodies, these normally recycling receptors are routed to lysosomes. This abnormal routing may be induced by receptor aggregation since cells treated with non-cross-linking monovalent antibodies to the ASGP receptor (Schwartz et al., 1986), LDL receptor (Anderson et al., 1982), and Fc receptor (Mellman et al., 1984), show normal receptor routing.

An iterative fractionation process in a sorting endosome provides a simple mechanism for the process of endocytic sorting, one that is consonant with what is known about the kinetics and cellular structures involved in endocytic sorting. The data we present are consistent with those of other studies and support several of the specific predictions of this model. Studies are presently underway to further characterize the process and structures involved in the endosomal accumulation of LDL and recycling of Tf.

We thank Michael Hillmeyer and Raj Kumar for developing software for the automated digital image processing procedures. We thank Peter Marks for technical assistance and Nita Salzman and Karsten Fliegner for their helpful discussion and suggestions. We also thank Michael Koval and Richard Pagano for providing us with their results before publication.

This work was supported by National Institutes of Health (NIH) grant DK 27083 (to F. Maxfield) and NIH fellowship F32 GM12148 (to K. Dunn).

Received for publication 27 April 1989 and in revised form 13 September 1989.

References

Ajioka, R. S., and J. Kaplan. 1987. Intracellular pools of transferrin receptors result from constitutive internalization of unoccupied receptors. *Proc. Natl. Acad. Sci. USA.* 83:6445-6449.

Anderson, R. G. W., M. S. Brown, U. Beisiegel, and J. L. Goldstein. 1982. Surface distribution and recycling of the LDL receptor as visualized by anti-receptor antibodies. *J. Cell Biol.* 93:523-531.

Braell, W. A. 1981. Fusion between endocytic vesicles in a cell free system. *Proc. Natl. Acad. Sci. USA.* 84:1137-1141.

Breitfeld, P. P., C. F. Simmons, G. J. Strous, H. J. Geuze, and A. L. Schwartz. 1985. Cell biology of the asialoglycoprotein system: a model of receptor-mediated endocytosis. *Int. Rev. Cytol.* 97:47-95.

Brown, M. S., R. G. W. Anderson, and J. L. Goldstein. 1983. Recycling receptors: the round trip itinerary of migrant membrane proteins. *Cell.* 32:663-667.

Burgert, H. G., and L. Thilo. 1983. Internalization and recycling of plasma membrane glycoconjugates during pinocytosis in the macrophage cell line p388D_1. *Exp. Cell Res.* 144:127-142.

Carpenter, G., and S. Cohen. 1979. Epidermal growth factor. *Annu. Rev. Biochem.* 48:193-216.

Dautry-Varsat, A., A. Ciechanover, and H. F. Lodish. 1983. pH and the recycling of transferrin during receptor-mediated endocytosis. *Proc. Natl. Acad. Sci. USA.* 80:2258-2262.

Diaz, R., L. Mayorga, and P. Stahl. 1988. In vitro fusion of endosomes following receptor-mediated endocytosis. *J. Biol. Chem.* 263:6093-6100.

Draper, R. K., and M. I. Simon. 1980. The entry of diphtheria toxin in to the mammalian cell cytoplasm: evidence for lysosomal involvement. *J. Cell Biol.* 87:849-854.

Duncan, R., and M. K. Pratten. 1977. Membrane economics in endocytic systems. *J. Theor. Biol.* 66:727-735.

Fuller, S. D., and K. Simons. 1986. Transferrin receptor polarity and recycling accuracy in "tight" and "leaky" strains of Madin-Darby canine kidney cells. *J. Cell Biol.* 103:1767-1779.

Geuze, H. J., J. W. Slot, G. J. A. M. Strous, H. F. Lodish, and A. L. Schwartz. 1983. Intracellular site of asialoglycoprotein receptor-ligand uncoupling: double label immunoelectron microscopy during receptor mediated endocytosis. *Cell.* 32:277-287.

Geuze, H. J., J. W. Slot, and A. L. Schwartz. 1987. Membranes of sorting organelles display lateral heterogeneity in receptor distribution. *J. Cell Biol.* 104:1715-1723.

Goldstein, J. L., S. K. Basu, and M. S. Brown. 1983. Receptor mediated endocytosis of low-density lipoprotein in cultured cells. *Methods Enzymol.* 98:241-260.

Goldstein, J. L. M. S. Brown, R. G. W. Anderson, D. W. Russell, and W. J. Schneider. 1985. Receptor mediated endocytosis: concepts emerging from the LDL receptor system. *Annu. Rev. Cell Biol.* 1:1-39.

Greenspan, P., and R. W. St. Clair. 1984. Retroendocytosis of low density lipoprotein: effect of lysosomal inhibitors on the release of undegraded ^{125}I-low density lipoprotein of altered composition from skin fibroblasts in culture. *J. Biol. Chem.* 259:1703-1713.

Gruenberg, J. E., and K. E. Howell. 1986. Reconstitution of vesicle fusions occurring in endocytosis with a cell free system. *EMBO (Eur. Mol. Biol. Organ.) J.* 5:3091-3101.

Haigler, H. T., F. R. Maxfield, M. C. Willingham, and I. Pastan. 1980. Dansylcadaverine inhibits internalization of ^{125}I-epidermal growth factor in BALB 3T3 cells. *J. Biol. Chem.* 255:1239-1241.

Harford, J., K. Bridges, G. Ashwell, and R. D. Klausner. 1983*a*. Intracellular dissociation of receptor-bound asialoglycoproteins in cultured hepatocytes: a pH-mediated nonlysosomal event. *J. Biol. Chem.* 258:3191-3197.

Harford, J., A. W. Wolkoff, G. Ashwell, and R. D. Klausner. 1983*b*. Monensin inhibits intracellular dissociation of asialoglycoproteins from their receptor. *J. Cell Biol.* 96:1824-1828.

Hopkins, C. R., and I. S. Trowbridge. 1983. Internalization and processing of transferrin and the transferrin receptor in human carcinoma A4331 cells. *J. Cell Biol.* 97:508-521.

Kam, Z. 1987. Microscopic imaging of cells. *Q. Rev. Biophys.* 20:201-259.

Keen, J. H., F. R. Maxfield, M. C. Hardegree, and W. H. Habig. 1982. Receptor mediated endocytosis of diphtheria toxin by cells in culture. *Proc. Natl. Acad. Sci. USA.* 79:2912-2916.

Klausner, R. D., G. Ashwell, J. Van Renswoude, J. B. Harford, and K. R. Bridges. 1983. Binding of apotransferrin to K562 cells: explanation of the transferrin cycle. *Proc. Natl. Acad. Sci. USA.* 80:2263-2266.

Koval, M., and R. E. Pagano. 1989. Lipid recycling between the plasma membrane and intracellular compartments: transport and metabolism of fluorescent sphingomyelin analogs in cultured fibroblasts. *J. Cell Biol.* 108:2169-2181.

Linderman, J. L., and D. A. Lauffenburger. 1988. Analysis of intracellular receptor/ligand sorting in endosomes. *J. Theor. Biol.* 132:203-245.

Marsh, M., E. Bolzau, and A. Helenius. 1983. Penetration of Semliki forest virus from acidic prelysosomal vacuoles. *Cell.* 32:931-940.

Maxfield, F. R. 1989. Measurement of vacuolar pH and cytoplasmic calcium in living cells using fluorescence microscopy. *Methods Enzymol.* 173:745-771.

Maxfield, F. R., J. Schlessinger, Y. Shector, I. Pastan, and M. C. Willingham. 1978. Collection of insulin, EGF, and α-2-macroglobulin in the same patches on the surface of cultured fibroblasts and common internalization. *Cell.* 14:805-810.

Maxfield, F. R., and K. W. Dunn. 1989. Studies of endocytosis using image intensification fluorescence microscopy and digital image analysis. *In* Digitized Video Microscopy. B. Herman and K. Jacobson, editors. Alan R. Liss Inc., New York. In press.

McGraw, T. E., L. Greenfield, and F. R. Maxfield. 1987. Functional expression of the human transferrin receptor cDNA in Chinese hamster ovary cells deficient in endogenous transferrin receptor. *J. Cell Biol.* 105:207-214.

Mellman, I. S., and H. Plutner. 1984. Internalization and fate of macrophage Fc receptors bound to polyvalent immune complexes. *J. Cell Biol.* 98: 1170-1177.

Mellman, I., H. Plutner, and P. Ukkonen. 1984. Internalization and rapid recycling of macrophage Fc receptors tagged with monovalent antireceptor antibody: possible role of a prelysosomal compartment. *J. Cell Biol.* 98:1163-1169.

Mostov, K. E., M. Friedlander, and G. Blobel. 1984. The receptor for transepithelial transport of IgA and IgM contains multiple immunoglobulin-like domains. *Nature (Lond.).* 308:37-43.

Olsnes, S., and K. Sandvig. 1985. Entry of polypeptide toxins into animal cells. *In* Endocytosis. I. Pastan, and M. C. Willingham, editors. Plenum Publishing Corp., New York. 195-234.

Omary, M. B., and I. S. Trowbridge. 1981. Biosynthesis of the human transferrin receptor. *J. Biol. Chem.* 256:12888-12892.

Pastan, I., and M. C. Willingham. 1983. Receptor mediated endocytosis: coated pits, receptosomes and the Golgi. *Trends Biochem. Sci.* 8:250-254.

Pitas, R. E., T. L. Innerarity, J. N. Weinstein, and R. W. Mahley. 1981. Acetoacetylated lipoproteins used to distinguish fibroblasts from macrophages *in vitro* by fluorescence microscopy. *Arteriosclerosis.* 1:177-185.

Raub, T. J., J. B. Denny, and R. M. Roberts. 1986. Cell surface glycoproteins of CHO cells 1. Internalization and rapid recycling. *Exp. Cell Res.* 165: 73-91.

Rome, L. H. 1985. Curling receptors. *Trends Biochem. Sci.* 10:151.

Salzman, N. H., and F. R. Maxfield. 1988. Intracellular fusion of sequentially formed endocytic compartments. *J. Cell Biol.* 106:1083-1091.

Salzman, N. H., and F. R. Maxfield. 1989. Fusion-accessibility of endocytic compartments along the recycling and lysosomal endocytic pathways in in-

tact cells. *J. Cell Biol.* 109:2097–2104.
Schlessinger, J. 1986. Allosteric regulation of the epidermal growth factor receptor kinase. *J. Cell Biol.* 103:2067–2072.
Schmid, S. L., R. Fuchs, P. Male, and I. Mellman. 1988. Two distinct subpopulations of endosomes involved in membrane recycling and transport to lysosomes. *Cell.* 52:73–83.
Schwartz, A. L., and D. Rup. 1983. Biosynthesis of the human asialoglycoprotein receptor. *J. Biol. Chem.* 258:11249–11255.
Schwartz, A. L., A. Ciechanover, S. Merritt, and A. Turkewitz. 1986. Antibody-induced receptor loss: different fates for asialoglycoproteins and the asialoglycoprotein receptor in HepG2 cells. *J. Biol. Chem.* 261:15225–15232.
Simmons, C. F., and A. L. Schwartz. 1984. Cellular pathways of galactose-terminal ligand movement in a cloned human hepatoma cell line. *Mol. Pharmacol.* 26:509–519.
Steinman, R. M., I. S. Mellman, W. A. Muller, and Z. A. Cohn. 1983. Endocytosis and recycling of plasma membrane. *J. Cell Biol.* 96:1–27.
Stoorvogel, W., H. J. Geuze, and G. J. Strous. 1987. Sorting of endocytosed transferrin and asialoglycoprotein occurs immediately after internalization in HepG2 cells. *J. Cell Biol.* 104:1261–1268.
Tycko, B., C. H. Keith, and F. R. Maxfield. 1983. Rapid acidification of endocytic vesicles containing asialoglycoprotein in cells of a human hepatoma line. *J. Cell Biol.* 97:1762–1776.
Van Leuven, F., J.-J. Cassiman, and H. Van Den Berghe. 1980. Primary amines inhibit recycling of α_2M receptors in fibroblasts. *Cell.* 20:37–43.
Von Figura, K. V., V. Gieselmann, and A. Hasilik. 1984. Antibody to mannose 6 phosphate specific receptor induces receptor deficiency in human fibroblasts. *EMBO (Eur. Mol. Biol. Organ.) J.* 3:1281–1286.
Ward, D. M., R. Ajioka, and J. Kaplan. 1989. Cohort movement of different ligands and receptors in the intracellular endocytic pathway of alveolar macrophages. *J. Biol. Chem.* 264:8164–8170.
Weigel, P. H., and J. A. Oka. 1984. Recycling of the hepatic asialoglycoprotein receptor in isolated rat hepatocytes. *J. Biol. Chem.* 259:1150–1154.
Weissman, A. M., R. D. Klausner, K. Rao, and J. B. Harford. 1986. Exposure of K562 cells to anti-receptor monoclonal antibody OKT9 results in rapid redistribution and enhanced degradation of the transferrin receptor. *J. Cell Biol.* 102:951–958.
Yamashiro, D. J., B. Tycko, S. R. Fluss, and F. R. Maxfield. 1984. Segregation of transferrin to a mildly acidic (pH 6.5) para-Golgi compartment in the recycling pathway. *Cell.* 37:789–800.